12. Materials and methods are available as supporting material on *Science* Online.
13. M. Haruta, *Catal. Today* **36**, 153 (1997).
14. A. Abad, P. Concepcion, A. Corma, H. Garcia, *Angew. Chem. Int. Ed.* **44**, 4066 (2005).
15. D. I. Enache *et al.*, *Science* **311**, 362 (2006).
16. J. C. Scaiano, S. García, H. García, *Tetrahedron Lett.* **38**, 5929 (1997).
17. O. Brede, A. Maroz, R. Hermann, S. Naumov, *J. Phys. Chem. A* **109**, 8081 (2005).
18. M. Oyama, M. Goto, *Indian J. Chem. Sect. A* **42A**, 733 (2003).
19. W. Hub, S. Schneider, F. Doerr, J. D. Oxman, F. D. Lewis, *J. Am. Chem. Soc.* **106**, 701 (1984).
20. W. Hub, S. Schneider, F. Doerr, J. D. Oxman, F. D. Lewis, *J. Phys. Chem.* **87**, 4351 (1983).
21. E. Lamy-Pitara, B. N' Zemba, J. Barbier, F. Barbot, L. Miginiac, *J. Mol. Catal. Al* **142**, 39 (1999).
22. S. Carrettin *et al.*, *Chem. Eur. J.* **13**, 7771 (2007).
23. Financial support by the Spanish DGI (MAT06-14274-C02-01 and CTQ2006-0658) is gratefully acknowledged. A.G. thanks the Spanish CSIC for a JAE research associate contract. A patent covering the use of these catalysts for the aerobic synthesis of azo benzenes has been filed at the Spanish Patent Office.

Supporting Online Material
www.sciencemag.org/cgi/content/full/322/5908/1661/DC1
Materials and Methods
Figs. S1 to S3
Table S1

25 September 2008; accepted 14 November 2008
10.1126/science.1166401

Collective Reactivity of Molecular Chains Self-Assembled on a Surface

Peter Maksymovych,[1,2] Dan C. Sorescu,[3] Kenneth D. Jordan,[1] John T. Yates Jr.[1,4]*

Self-assembly of molecules on surfaces is a route toward not only creating structures, but also engineering chemical reactivity afforded by the intermolecular interactions. Dimethyldisulfide (CH_3SSCH_3) molecules self-assemble into linear chains on single-crystal gold surfaces. Injecting low-energy electrons into individual molecules in the self-assembled structures with the tip of a scanning tunneling microscope led to a propagating chemical reaction along the molecular chain as sulfur–sulfur bonds were broken and then reformed to produce new CH_3SSCH_3 molecules. Theoretical and experimental evidence supports a mechanism involving electron attachment followed by dissociation of a CH_3SSCH_3 molecule and initiation of a chain reaction by one or both of the resulting CH_3S intermediates.

Self-assembled molecular structures on metal and semiconductor surfaces (*1*, *2*) can produce properties that are not observed in isolated adsorbed molecules. For example, the proximity of atoms or molecules can allow their electronic states to delocalize (*3*–*6*), leading to increased electron mobility in the overlayer that can be desirable for potential applications in molecular electronics and organic solar cells (*7*). Other functionalities that are enabled by self assembly include molecular cascades within prearranged molecules (*8*), directional polymerization (*9*), switching of electronic states of surface adatoms in molecular corrals (*10*), and the tunable confinement of electronic surface states in supramolecular gratings (*11*).

Here we report that chemical reactivity can also be induced by self-assembly. A linear chain of molecules (CH_3SSCH_3) adsorbed on a gold surface has been found to respond collectively to electron attachment and undergo a chemical reaction that involves S–S bond dissociation and recombination reactions extending throughout the molecular assembly. The molecular self-alignment reduces the activation energy to break the S–S bond of the CH_3SSCH_3 molecule inside the assembly by at least a factor of 5, allowing for the facile propagation of the chain reaction through as many as 10 neighboring molecules [on the Au(100) surface] before being quenched. The self-assembled molecular structure thus redirects the energy flow toward a chemical chain reaction involving multiple steps, rather than rapid dissipation into the metal bulk.

We have studied electron-induced reactions of CH_3SSCH_3 molecules bonded to Au(111) and Au(100) surfaces using scanning tunneling microscopy (STM) at 5 K to inject electrons and image the reaction products [see supporting online material (SOM)]. Single molecules adsorb on the Au(111) surface with a calculated binding energy of 11.8 kcal/mol in a structural geometry shown in Fig. 1A (*12*). Methyl groups located at the two ends of the S–S bond assume a trans conformation. We observed a total of six equivalent orientations of isolated CH_3SSCH_3 molecules (two mirror images for each of three azimuthal orientations) on the Au(111) surface. At a higher molecular coverage and at adsorption temperatures between 70 and 200 K, "linear" CH_3SSCH_3 chains up to five units in length form on the Au(111) surface. The epitaxial chains run along the $<11\bar{2}>$ crystallographic direction with a periodicity of 0.5 nm (Fig. 1, B and C). Every molecule in the chain has the same orientation of the S–S

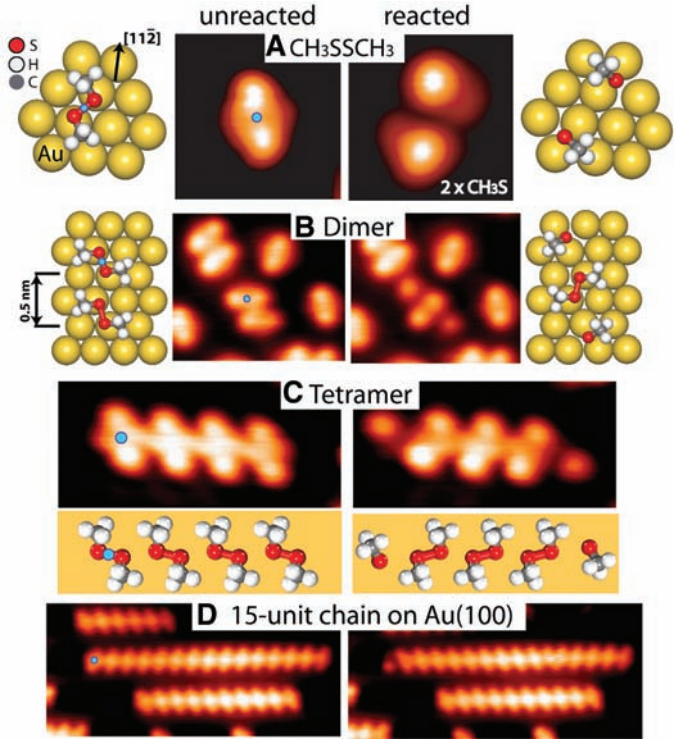

Fig. 1. STM images before and after electron-induced dissociation of a single CH_3SSCH_3 molecule and the self-assembled chains on the Au(111) surface. Schematic ball models of the selected structures are shown aside their STM images. (**A**) Dissociation of CH_3SSCH_3 producing two CH_3S fragments by a pulse of tunneling current at 1.4 V (*12*). (**B** and **C**) Chain reactions in CH_3SSCH_3 dimer and tetramer assemblies on Au(111) induced by a voltage pulse on top of the terminal molecule (blue dot, pulse voltage 0.9 V), leading to the synthesis of CH_3SSCH_3 molecules of opposite conformation. (**D**) A similar chain reaction on the Au(100) surface that involves 10 out of 15 molecules in a row and produces 9 new CH_3SSCH_3 molecules.

[1]Department of Chemistry and Center for Molecular and Materials Simulations, University of Pittsburgh, Pittsburgh, PA 15260, USA. [2]Center for Nanophase Materials Sciences, Oak Ridge National Laboratory, Oak Ridge, TN 37831, USA. [3]U.S. Department of Energy, National Energy Technology Laboratory, Pittsburgh, PA 15236, USA. [4]Department of Chemistry, University of Virginia, Charlottesville, VA 22904, USA.

*To whom correspondence should be addressed. E-mail: johnt@virginia.edu

Report Documentation Page

Form Approved
OMB No. 0704-0188

1. REPORT DATE	2. REPORT TYPE	3. DATES COVERED
2008		**00-00-2008 to 00-00-2008**

4. TITLE AND SUBTITLE	5a. CONTRACT NUMBER
Collective Reactivity of Molecular Chains Self-Assembled on a Surface	**W911NF-04-1-0200**
	5b. GRANT NUMBER
	5c. PROGRAM ELEMENT NUMBER
6. AUTHOR(S)	5d. PROJECT NUMBER
	5e. TASK NUMBER
	5f. WORK UNIT NUMBER
7. PERFORMING ORGANIZATION NAME(S) AND ADDRESS(ES) **Department of Chemistry and Center for Molecular and Materials Simulations,,University of Pittsburgh,Pittsburgh,PA,15260**	8. PERFORMING ORGANIZATION REPORT NUMBER **; 45758-CH.10**
9. SPONSORING/MONITORING AGENCY NAME(S) AND ADDRESS(ES) **U.S. Army Research Office, P.O. Box 12211, Research Triangle Park, NC, 27709-2211**	10. SPONSOR/MONITOR'S ACRONYM(S)
	11. SPONSOR/MONITOR'S REPORT NUMBER(S) **45758-CH.10**

12. DISTRIBUTION/AVAILABILITY STATEMENT
Approved for public release; distribution unlimited
13. SUPPLEMENTARY NOTES
14. ABSTRACT
15. SUBJECT TERMS

16. SECURITY CLASSIFICATION OF:			17. LIMITATION OF ABSTRACT	18. NUMBER OF PAGES	19a. NAME OF RESPONSIBLE PERSON
a. REPORT	b. ABSTRACT	c. THIS PAGE			
unclassified	**unclassified**	**unclassified**	**Same as Report (SAR)**	**4**	

bond relative to the gold surface, as well as essentially the same trans configuration of the CH_3 groups. Density functional theory (DFT) calculations, described below, predict that the binding energy of the CH_3SSCH_3 molecules to the surface decreases by ~1 kcal/mol upon chain formation, which is consistent with the spontaneous chain growth only at a high molecular coverage.

The effect of electron injection is illustrated in Fig. 1 for the case of a single CH_3SSCH_3 molecule (Fig. 1A), a self-assembled dimer (Fig. 1B), and a tetramer (Fig. 1C) on the Au(111) surface. Electron injection into a single CH_3SSCH_3 molecule (blue circle, pulsed at 0.9 to 1.4 V, 1 to 2 nA, 10 to 100 ms) resulted in its dissociation into equivalent adsorbed CH_3S fragments (*12*), as shown in Fig. 1A. In contrast, similar excitation of the dimer and tetramer created new CH_3SSCH_3 molecules in the interior of the chain and formed one CH_3S entity at each end of the original chain, as seen from a detailed analysis of the electron injection–induced reaction of the tetramer in Fig. 2, A to C. Because we can determine the position of the molecules relative to the underlying surface lattice on the basis of the known crystallographic directions and the adsorption site of the CH_3SSCH_3 molecule (*13*), we infer that the CH_3SSCH_3 molecules produced in the electron-induced chain reactions were translated by ~2.5 Å, relative to the reactant molecules (Fig. 2, D and E).

The production of new CH_3SSCH_3 molecules in the chain's interior, the production of a CH_3S species at each end of the chain, and the 2.5 Å shift of the product species are consistent only with a reaction process where the S–S bonds of a series of CH_3SSCH_3 molecules in the chain are broken and new S–S bonds are formed, as shown schematically in Fig. 1, B and C, for the dimer and tetramer. The chain reaction can be envisioned as a sequence of elementary steps ($CH_3S + CH_3SSCH_3 \rightarrow CH_3SSCH_3 + CH_3S$), each of which is closely reminiscent of the photo-

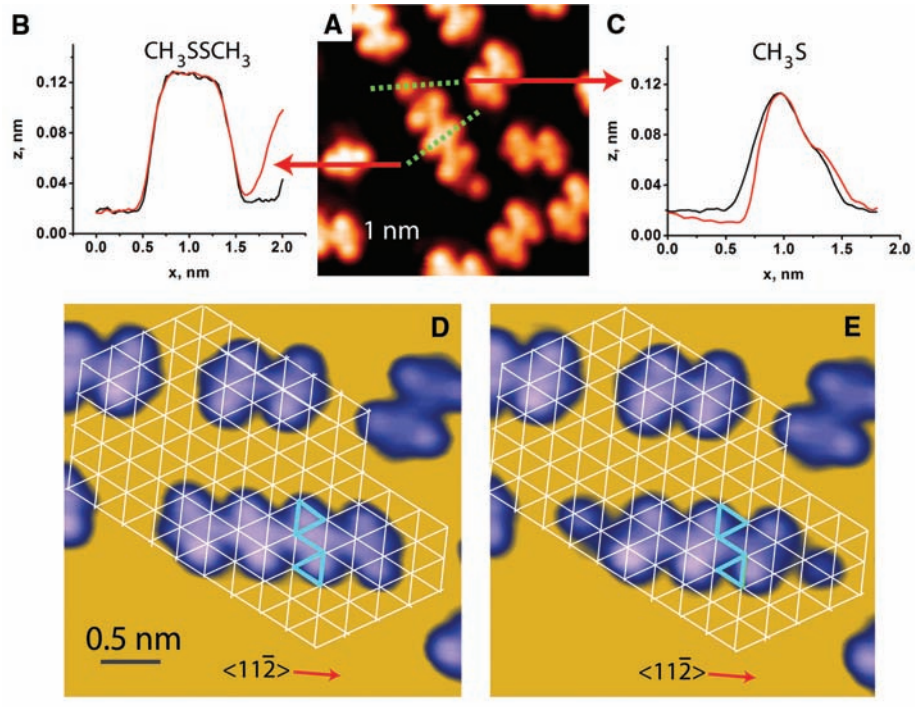

Fig. 2. Topographic analysis of the products of the chain reaction of the CH_3SSCH_3 tetramer on Au(111). (**A**) STM image of the reacted CH_3SSCH_3 tetramer. (**B**) Line profile of isolated CH_3SSCH_3 (black) compared with CH_3SSCH_3 in the middle of the reacted chain (red); the line profiles were taken along the corresponding green dashed lines in (A). (**C**) STM line profile of isolated CH_3S (black) compared with CH_3S at the end of the reacted chain (red). (**D** and **E**) Triangulation of CH_3SSCH_3 tetramer [surface lattice derived from studies of CH_3SSCH_3 adsorption (*13*)]. The product molecules are shifted by 2.5 Å along the <11$\bar{2}$> direction.

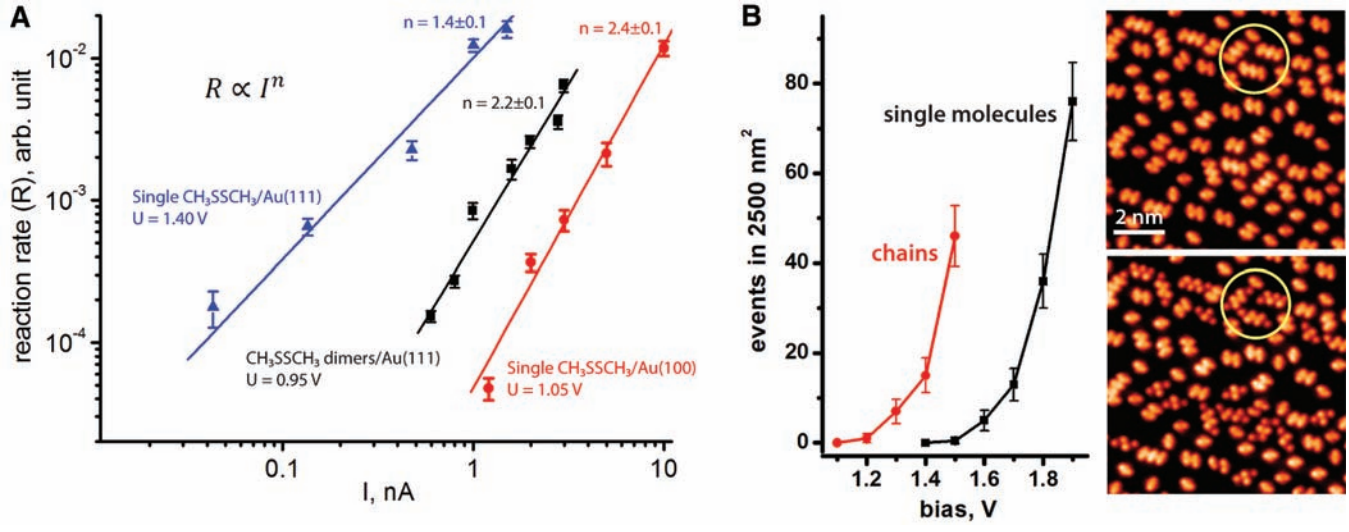

Fig. 3. (**A**) Kinetics of the chain reaction and single-molecule dissociation of CH_3SSCH_3 molecules on Au(111) and Au(100) surfaces obtained from statistical analysis of 100 to 200 single-molecule (chain) excitations. *n* is a slope of the least-squares fit of the reaction rate as a function of tunneling current in the log-log coordinates. Error bars are from fit to Poisson distribution. (**B**) Yield of the long-range reaction (*22*) as a function of the excitation energy for self-assembled chains (red) and single molecules (black) on Au(111). The excitation pulse (I = 20 pA, 1-s duration for both data sets) was applied at an uncovered point near the center of the field of view, and the reaction events were counted in the surrounding area of 2500 nm^2. Each point represents an average of one to three subsequent pulses. (Right) STM images showing the same area before and after several pulses with voltages up to 1.5 V. Many chains are observed to react (e.g., yellow circle with three trimers), whereas single molecules remain intact throughout the image. Error bars are from the square root of the even count, assuming a Gaussian distribution.

induced free-radical substitution reactions in the gas phase involving the thyil radical (RS•) (*14*). Although partial surface bonding of the intermediate CH_3S species (see below) differentiates it from a free radical, we believe that the chain process observed here represents the atomic-level observation of a radical-mediated chain reaction along the lines of the early postulates in the field of gas-phase kinetics (*15*).

As seen in Figs. 1 and 2, the new CH_3SSCH_3 molecules produced in the chain reaction are aligned in a different way relative to the gold lattice, as compared with the original molecules. The realignment can best be visualized as a reflection of the molecule in the mirror plane that runs perpendicular to the chain. A large number of measurements have shown that such realignment does not result from electron injection from the scanning tunneling microscope tip into isolated adsorbed CH_3SSCH_3 molecules; only S–S bond scission or diffusion of the whole molecule occurs (*12*). The chain reaction thus represents a new reaction coordinate for CH_3SSCH_3 molecules dissociating on a surface that appears by virtue of self-assembly. On Au(111), the twofold bonding sites are thermodynamically favorable for the CH_3S species (*13*), which makes them the sole product of single-molecule dissociation. However, the close packing of the CH_3SSCH_3 molecules in the self-assembled chains prevents binding of the nascent CH_3S to the twofold Au sites. Instead, the CH_3S fragment is made to react with a neighboring CH_3SSCH_3 molecule, and a chain reaction occurs in which CH_3S species induce the scission of neighboring S–S bonds. The DFT calculations (see below), predict that after the initial S–S bond-breaking event, subsequent steps proceed with zero or only very small energy barriers, resembling the control of the steric factor in surface processes initiated by electronic excitation on single-crystal templates, such as in surface-aligned photochemistry (*16*, *17*).

A chain reaction can also be induced by pulsing electrons into CH_3SSCH_3 molecules self-assembled on the Au(100) surface, and it is very similar to its analog on Au(111). As seen in Fig. 1D, the reaction of the 15-unit chain of CH_3SSCH_3 molecules on Au(100) produces a terminal CH_3S species, followed by 9 contiguous reoriented CH_3SSCH_3 molecules, and then another CH_3S species embedded in the partially reacted chain, thus involving a total of 10 CH_3SSCH_3 molecules. As on Au(111), the apparent tilt of the CH_3SSCH_3 molecules relative to chain direction is seen to be switched by the reaction, signaling the involvement of the S–S bond dissociation/recombination processes. The most likely cause for the incomplete reaction in the 15-unit chain is energy dissipation to the substrate during the sequence of thermo-neutral steps.

Insight into the process leading to the chain reaction comes from the measurement of the average single-molecule reaction rate as a function of the STM current, as described by W. Ho (*18*). As shown in Fig. 3A, the rate of a single CH_3SSCH_3 dissociation scales as the 1.4 ± 0.1th power of the current at a tunneling bias of 1.40 eV. We therefore interpret single-molecule dissociation to be a one-electron process. The quantum yield for the single-molecule reaction is at least 10^{-7} events per electron, which is several orders of magnitude higher than that found for surface reactions caused by direct vibrational excitation of the molecules by tunneling electrons (*18*–*20*). These observations support a mechanism involving electron capture into the lowest unoccupied molecular orbital (LUMO) of the adsorbed CH_3SSCH_3 molecule (*21*). This orbital is antibonding and localized on the S–S bond (Fig. 4A). The DFT calculations predict the LUMO to be centered at ~1.8 eV above the Fermi level (Fig. 4A), which, considering broadening of the levels and additional image-charge stabilization of the transient anion, is in good agreement with the observed reaction onset at 1.4 eV. After the electron capture, the reaction can proceed by either of two separate routes: (i) dissociation of the anion state, in which case the process is known as dissociative attachment (*21*), or (ii) electron detachment leaving a vibrationally hot CH_3SSCH_3 molecule, which then proceeds to dissociate. At present, we cannot determine which of these two processes is dominant.

One electron–induced dissociation of single CH_3SSCH_3 molecules is independently confirmed by a kinetic study of the long-range dissociation that occurs in a large area around the scanning tunneling microscope tip (up to 50-nm radius at 2.0 eV) if the electron energy exceeds 1.4 eV, as

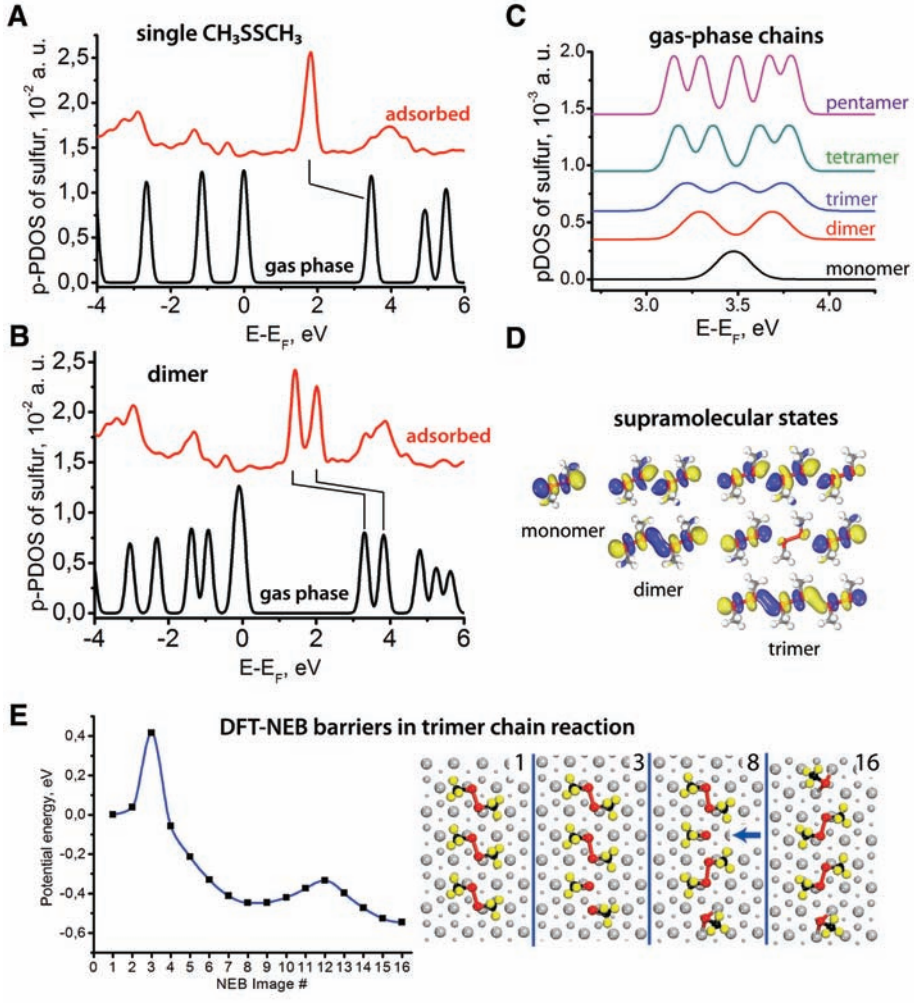

Fig. 4. Density of states projected onto p orbitals of sulfur atoms (p-PDOS) in (**A**) a single CH_3SSCH_3 molecule on Au(111) (red) and in the gas phase (black) and (**B**) a CH_3SSCH_3 dimer on Au(111) (red) and in the gas phase (black). (**C**) p-PDOS of sulfur atoms in the gas-phase assemblies of CH_3SSCH_3 molecules with peaks that correspond to low-lying supramolecular orbitals. The orbitals are shown for the monomer, dimer, and trimer. The structures used in calculations correspond to the equilibrium geometry of the adsorbed chains calculated in the slab models. (**D**) Representative supramolecular orbitals are shown for the dimer and trimer in the order of ascending energy from bottom to top. (**E**) Potential energy diagram calculated for the consecutive chain reaction scenario of the CH_3SSCH_3 trimer on Au(111) using DFT and NEB methods. Four representative NEB images are shown at right. The blue arrow in image 8 indicates the intermediate atop-bonded CH_3S species. a.u., arbitrary units; *E*, electron energy; E_F, Fermi energy.

detailed in (*22*). The long-range reaction is caused by hot electrons transported laterally via a surface resonance of Au(111). The chain reactions are observed to be similarly long-range (Fig. 3B) above a threshold excitation energy, identifying them as one-electron processes under these conditions. An important distinction between the long-range reactions involving single molecules and those involving CH_3SSCH_3 chains on the Au(111) [as well as the Au(100)] surface is a substantially lower (by >0.2 eV) energy threshold for the chain reaction, as determined from a statistical analysis of the long-range reactions (left panel in Fig. 3B). This observation is also confirmed by the STM images shown at the right in Fig. 3B, where several consecutive excitation pulses in the center of the STM image with a maximum energy of 1.5 eV cause multiple chain reactions in the surrounding area (for instance, trimers in the yellow circle), whereas all of the isolated molecules in the field of view remain intact.

Figure 4, A and B, provides the details of the calculated electronic structure of a single CH_3SSCH_3 molecule and the self-assembled dimer (see SOM), both in the gas phase (blue curves) and adsorbed on a four-layer slab of Au(111) (red curves). The purpose of the gas-phase calculations is to estimate the degree of molecular orbital overlap that can exist between CH_3SSCH_3 molecules positioned at a distance and in the orientation closest to their adsorbed state. Therefore the gas-phase species are frozen in their optimized adsorbed configuration. The major changes upon adsorption are: (i) the LUMOs shift downward in energy upon adsorption by ~1.6 eV (single molecule) and ~1.8 eV (dimer), and (ii) the LUMO of the monomer is split into two or more low-lying orbitals in the dimer and longer self-assembled chains (Fig. 4, C and D). In the tetramer chain, the LUMO is calculated to be 0.4 eV closer to the Fermi level than is the LUMO of an isolated CH_3SSCH_3 molecule (Fig. 4, A and B). This result explains the lower threshold energy (by >0.3 eV) (Fig. 3B) for the initiation of the chain reaction in the tetramer, as compared with that for dissociation of the isolated molecule. The LUMO-derived orbitals are considerably less broadened upon adsorption as compared with other molecular orbitals (Fig. 4, A and B), which implies that the former do not mix appreciably with the electronic states of the gold substrate (*23*). Direct imaging by STM of the LUMO of the isolated CH_3SSCH_3 molecules or their chains is not possible on gold surfaces because of the high efficiency of dissociation.

The chain reaction can also be induced by tunneling electrons at a substantially lower energy (i.e., 0.7 to 1.0 eV) than the 1.2-eV threshold reported in Fig. 3B, if the scanning tunneling microscope tip is positioned directly above a molecular unit of the chain, as in Fig. 1. In this case, the reaction is strictly localized to the chain under the scanning tunneling microscope tip, and the reaction rate scales approximately quadratically with tunneling current (Fig. 3A), establishing a two-electron mechanism (*19*). The energy of each electron is substantially higher than any of the fundamental frequencies of the CH_3SSCH_3 molecule [the highest of which is a C–H stretch with an energy of ~360 mV (*24*)], whereas at the same time it is about half as large as the onset energy for single-electron dissociation. Although this could signal a direct vibrational excitation process, the sharp increase of the reaction rate in the energy range between 0.7 and 1.0 eV suggests that the two-electron process may also proceed through an anionic intermediate, with the first electron causing direct vibrational excitation and the second being captured by a vibrationally hot CH_3SSCH_3 molecule.

How does the transient anion formed by electron attachment to a CH_3SSCH_3 chain on a gold surface evolve? In the case of the surface-resonance assisted excitation, the hot electron is captured by a delocalized orbital, as shown in Fig. 4. However, the initially formed delocalized anionic state is likely to become rapidly localized on an individual CH_3SSCH_3 molecule through vibronic coupling. When the tip is positioned directly above the chain, the resulting anion is expected to be initially localized on a single CH_3SSCH_3 molecule, because the molecule directly under the tip will probably be electronically decoupled from the chain by either the electric field of the tip or the vibrational excitation in the two-electron regime. In general, anion states on metal surfaces have very short (subfemtosecond) lifetimes (*25*). However, even with such a short lifetime, a small fraction of the CH_3SSCH_3 anions could dissociate before electron detachment. This possibility is intriguing because this process would be barrierless, whereas the DFT calculations give a barrier of ~0.4 eV for breaking the first S–S bond for the neutral chain. Otherwise, the molecule can dissociate in the ground electronic state if the neutralization of the anion provides enough vibrational excitation to the molecule.

The dissociation of either neutral or anionic CH_3SSCH_3 molecules at the end of a chain produces CH_3S fragments with considerable excess kinetic energy, one of which impinges on a neighboring CH_3SSCH_3 molecule, leading to cleavage of its S–S bond, the formation of a new S–S bond, and the ejection of another CH_3S fragment that can repeat the process. In the event that the initially cleaved CH_3SSCH_3 is in the interior of the chain, both CH_3S fragments induce reactions in the two directions along the chain, as has been observed experimentally after locally pulsing a molecule in the middle of the chain. Gradual dissipation of the kinetic energy to the underlying bulk eventually quenches the chain reaction. We calculated the energy landscape for such a scenario for the neutral trimer assembly (Fig. 4E) and found that the barrier for breaking the first S–S bond is ~0.4 eV [nudged-elastic band (NEB) images 0 to 3)], as mentioned above, and that the S–S bond shifting process (NEB images 4 to 8) then proceeds without barriers. A small second barrier (~0.1 eV) in Fig. 4E is associated with the motion of the terminal CH_3S group toward its bridge-bonded site. The main reason for the nearly activationless interior reaction is the formation of a metastable complex, where an intermediate atop-bonded CH_3S species is stabilized by the neighboring CH_3SSCH_3 molecule.

The discovery of electron-induced chain reactions on surfaces suggests a number of future research directions. In addition to exploring the intriguing reaction dynamics in these systems with the use of ultrafast techniques, one can envision designer molecular assemblies on surfaces where chain reactions yield the desired final product via low-energy and stereospecific pathways. Also, the broad field of photochemistry on surfaces (*26*) will now have to account for chain processes in surface reaction mechanisms and in photocatalyst degradation.

References and Notes

1. J. V. Barth, G. Costantini, K. Kern, *Nature* **437**, 671 (2005).
2. G. M. Whitesides, B. Grzybowski, *Science* **295**, 2418 (2002).
3. L. Scifo *et al*., *Nano Lett.* **6**, 1711 (2006).
4. R. Temirov, S. Soubatch, A. Luican, F. S. Tautz, *Nature* **444**, 350 (2006).
5. M. Akai-Kasaya, K. Shimizu, Y. Watanabe, M. Aono, Y. Kuwahara, *Phys. Rev. Lett.* **91**, 255501 (2003).
6. N. Nilius, T. M. Wallis, W. Ho, *Science* **297**, 1853 (2002); published online 22 August 2002 (10.1126/science.1075242).
7. X.-Y. Zhu, *Surf. Sci. Rep.* **56**, 1 (2004).
8. A. J. Heinrich, C. P. Lutz, J. A. Gupta, D. M. Eigler, *Science* **298**, 1381 (2002); published online 24 October 2002 (10.1126/science.1076768).
9. Y. Okawa, M. Aono, *Nature* **409**, 683 (2001).
10. K. R. Harikumar, J. C. Polanyi, P. A. Sloan, S. Ayissi, W. A. Hofer, *J. Am. Chem. Soc.* **128**, 16791 (2006).
11. Y. Pennec *et al*., *Nat. Nanotechnol.* **2**, 99 (2007).
12. P. Maksymovych, J. T. Yates Jr., *J. Am. Chem. Soc.* **128**, 10642 (2006).
13. P. Maksymovych, D. C. Sorescu, J. T. Yates Jr., *J. Phys. Chem. B* **110**, 21161 (2006).
14. D. D. Carlson, A. R. Knight, *Can. J. Chem.* **51**, 1410 (1973).
15. M. Polanyi, *Atomic Reactions* (Williams and Norgate, London, 1932).
16. J. B. Giorgi, R. Kuhnemuth, J. C. Polanyi, *J. Chem. Phys.* **113**, 807 (2000).
17. C. E. Tripa, J. T. Yates Jr., *Nature* **398**, 591 (1999).
18. W. Ho, *J. Chem. Phys.* **117**, 11033 (2002).
19. H. Ueba, T. Mii, N. Lorente, B. N. J. Persson, *J. Chem. Phys.* **123**, 084707 (2005).
20. Y. Sainoo *et al*., *Phys. Rev. Lett.* **95**, 246102 (2005).
21. C. D. Lindstrom, X.-Y. Zhu, *Chem. Rev.* **106**, 4281 (2006).
22. P. Maksymovych, D. B. Dougherty, X.-Y. Zhu, J. T. Yates Jr., *Phys. Rev. Lett.* **99**, 016101 (2007).
23. K. J. Franke *et al*., *Phys. Rev. Lett.* **100**, 036807 (2008).
24. Y. Sainoo *et al*., *Phys. Rev. Lett.* **95**, 246102 (2005).
25. L. Bartels *et al*., *Phys. Rev. Lett.* **80**, 2004 (1998).
26. J. T. Yates Jr., H. Petek, *Chem. Rev.* **106**, 4113 (2006).

27. We thank D. B. Dougherty for fruitful discussions. P.M. and J.T.Y were supported by the W. M. Keck Foundation and the Army Research Office, and K.D.J acknowledges support from NSF through grant CHE0518253. A grant of computer time at the Pittsburgh Supercomputer Center is gratefully acknowledged. P.M. performed part of this research as a Eugene P. Wigner Fellow and staff member at the Oak Ridge National Laboratory, managed by UT-Battelle, for the U.S. Department of Energy under contract DE-AC05-00OR22725.

Supporting Online Material

www.sciencemag.org/cgi/content/full/322/5908/1664/DC1
SOM Text
References

29 August 2008; accepted 13 November 2008
10.1126/science.1165291